

Sub-picosecond proton tunnelling in deformed DNA hydrogen bonds under an asymmetric double-oscillator model

03/06/2022

J. LUO*

*jingxi.luo@durham.ac.uk

Department of Mathematical Sciences, Durham University

ABSTRACT

We present a model of proton tunnelling across DNA hydrogen bonds, compute the characteristic tunnelling time (CTT) from donor to acceptor and discuss its biological implications. The model is a double oscillator characterised by three geometry parameters describing planar deformations of the H bond, and a symmetry parameter representing the energy ratio between ground states in the individual oscillators. If the symmetry parameter takes its maximum value of 1, then we recover a known model which produced CTTs too large to be biologically relevant; but this is reduced by up to 40 orders of magnitude as the symmetry parameter is decreased. We discover that unless the symmetry parameter is close to 1 or 0, the proton's CTT under any planar deformation is guaranteed to be below one picosecond, which is a biologically relevant time-scale. This supports theories of links between proton tunnelling and biological processes such as spontaneous mutation.

1 Introduction

In the DNA double helix, the two strands of nucleobases are held together by hydrogen bonds, each consisting of a proton being covalently bonded with a donor atom from a donor molecule, and electrostatically attracted to an acceptor atom from an acceptor molecule [1, 2]. Löwdin proposed that the proton in an H bond may break away from the donor atom and form a new covalent bond with the acceptor atom, by the mechanism of quantum tunnelling across the potential barrier between the donor and acceptor, and that this process may cause spontaneous mutation [3]. McFadden and Al-Khalili later demonstrated that quantum coherence between the tunnelling proton and its environment can be maintained for biological time-scales, which validates modelling the proton’s dynamics as being entirely quantum mechanical [4].

In a *normal* H bond, all atoms in the donor and acceptor molecules are co-planar, and the donor and acceptor atoms are co-linear with the proton. A planar deformation of the normal H bond is some combination of translations and rotations in the donor-acceptor molecular plane [5–7]. It has been theorised that planar deformations of the H bond can have significant effects on the characteristic time-scale of proton tunnelling, and Krasilnikov studied these effects by modelling the potential in the H bond as a double harmonic oscillator which, when the bond is normal, is symmetric about the potential barrier [8]. It was found that the characteristic tunnelling time (CTT) of the proton was extremely sensitive to bond deformation, taking values up to $\mathcal{O}(10^{27})$ s, which was not a biologically relevant time-scale.

We propose a generalisation to Krasilnikov’s model, in which we associate the symmetry of the double-well potential in a normal H bond with a parameter, γ , whose value equals the energy ratio between a ground-state proton covalently bonded with the donor and one covalently bonded with the acceptor. When γ takes its maximum value of 1, we recover Krasilnikov’s model; when $0 < \gamma < 1$, the two local wells in the H bond potential are not equivalent, and the proton has a preferred equilibrium state near the donor rather than acceptor. We further encode the planar deformation of the H bond in three other parameters, d_x, d_y representing relative shifts between the donor and acceptor, and θ representing the relative rotation, all of which are defined in detail in Section 2. We then derive an analytical expression for the proton’s CTT. Fixing all other parameters such as proton mass and covalent bond lengths at values appropriate to DNA H bonds, the CTT is a function of γ, d_x, d_y and θ . We discover that moderate values of γ guarantee sub-picosecond proton tunnelling, regardless of bond deformation. In Section 3, we discuss the biological implications of our results.

2 Model and Results

In this Section, we firstly describe the geometry of an H bond under planar deformation, then define our double-well potential within this H bond, before solving the Schrödinger equation under this potential to obtain the proton’s wavefunction. From this wavefunction, we derive the proton’s CTT. We make the following assumptions and approximations in our model. Firstly, we consider only *stationary* bonds, meaning that the bond is not actively undergoing deformation whilst proton dynamics is taking place. Secondly, we assume that the lengths and relative angles of all *covalent* bonds in the donor and acceptor molecules are unaffected by the deformation. In other words, we only consider translations and rotations of the donor molecule as a whole and, independently, of the acceptor molecule as a whole. Finally, even though the proton’s global equilibrium is in a covalent bond with the donor atom, we assume that the proton can exist with a higher energy in a locally-stable state of being covalently bonded to

the acceptor atom. That there are two local potential minima for the proton in the H bond is the foundation of our double-oscillator model.

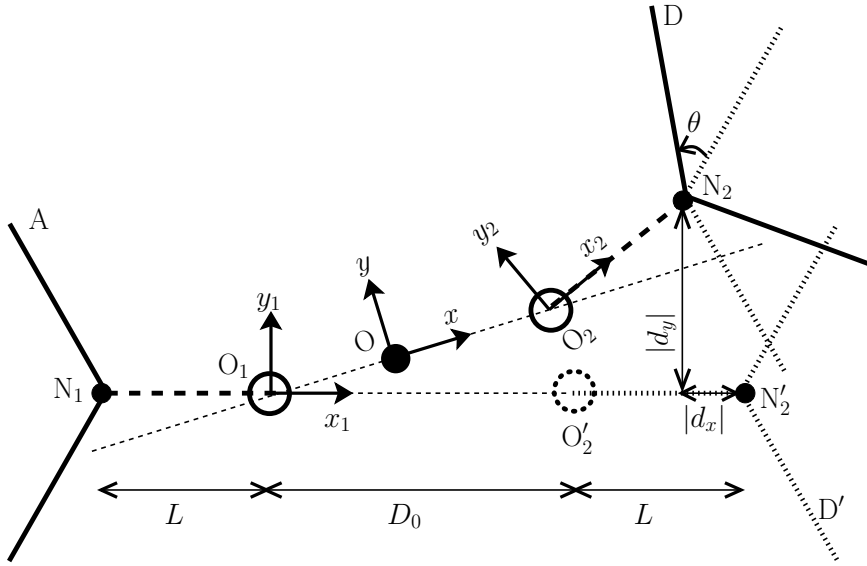


Figure 1: Geometry of a DNA H bond under planar deformation.

Since the H bond is planar, it suffices to model the potential for the proton as a function of two spatial dimensions. The geometry of the deformed H bond is shown in Figure 1. Thick lines marked A and D represent, respectively, the acceptor and donor molecules in a deformed bond, whilst the dotted line D' marks where the donor molecule would be in a normal bond. N₁ and N₂ mark the acceptor and donor atoms, respectively, and N₂' marks where the donor atom would be in a normal bond. We set up three Cartesian coordinate systems as follows. Firstly, centred at O₁, where a proton could exist in a covalent bond with N₁, we have (x₁, y₁), with x₁ pointing in the $\overrightarrow{N_1O_1}$ direction. Secondly, centred at O₂, where a proton could exist in a covalent bond with N₂, we have (x₂, y₂), with x₂ pointing in the $\overrightarrow{O_2N_2}$ direction. Lastly, centred at O, the saddle point in the double-well potential of the H bond, whose exact position along $\overrightarrow{O_1O_2}$ depends upon our potential function, we have (x, y), with x pointing in the $\overrightarrow{O_1O_2}$ direction. O₂' marks where O₂ would be in a normal bond. The bond geometry is entirely characterised by 5 parameters, which are marked in Figure 1 as L, D₀, d_x, d_y, θ , and defined as follows. L is the distance between N₁ and O₁, which we assume to be the same as the distance between N₂ and O₂, as well as the distance between N₂' and O₂', since we have assumed that no deformation affects the lengths of covalent bonds. D₀ is the distance between O₁ and O₂', in a normal bond. d_x and d_y are, respectively, the shifts in the x₁ and y₁ directions of the donor molecule from its normal position, so that, for instance, d_x < 0 represents a shift of the donor molecule *towards* the acceptor molecule. Finally, θ is the anticlockwise angle by which the donor molecule is rotated from its normal orientation, about the point N₂. We emphasise that the shifts are independent from the rotation, which means that the order in which d_x, d_y and θ act on the system does not affect its final configuration.

By comparing the coordinates of an arbitrary point in the three systems, O₁x₁y₁, O₂x₂y₂ and Oxy, we write down the following coordinate transformation equations.

$$x_1 = (x + \lambda D_\theta) \cos \theta_1 - y \sin \theta_1, \quad (1a)$$

$$y_1 = (x + \lambda D_\theta) \sin \theta_1 + y \cos \theta_1, \quad (1b)$$

$$x_2 = (x - (1 - \lambda) D_\theta) \cos \theta_2 - y \sin \theta_2, \quad (1c)$$

$$y_2 = (x - (1 - \lambda) D_\theta) \sin \theta_2 + y \cos \theta_2, \quad (1d)$$

where θ_1 is the anticlockwise angle from x_1 to x , θ_2 is the anticlockwise angle from x_2 to x , D_θ is the distance between O_1 and O_2 in the deformed bond, and λD_θ where $0 < \lambda < 1$ is the distance between O_1 and O in the deformed bond. We express $\theta_1, \theta_2, D_\theta$ and λ in terms of L, D_0, d_x, d_y and θ as follows.

$$\theta = 2\pi + \theta_1 - \theta_2, \quad (2a)$$

$$D_\theta \cos \theta_1 = D_0 + L + d_x - L \cos \theta, \quad (2b)$$

$$D_\theta \sin \theta_1 = d_y - L \sin \theta, \quad (2c)$$

which imply

$$D_\theta = \sqrt{[D_0 + d_x + L(1 - \cos \theta)]^2 + [d_y - L \sin \theta]^2} \quad (3a)$$

$$\cos \theta_1 = \frac{D_\theta}{D_0 + d_x + L(1 - \cos \theta)}, \quad \sin \theta_1 = \frac{D_\theta}{d_y - L \sin \theta}, \quad (3b)$$

$$\cos \theta_2 = \cos \theta_1 \cos \theta + \sin \theta_1 \sin \theta, \quad \sin \theta_2 = \sin \theta_1 \cos \theta - \cos \theta_1 \sin \theta, \quad (3c)$$

and λ is dependent upon the form of the potential function over the (x, y) plane. For our asymmetric double-oscillator model, we consider a potential function $V = V_1 + V_2$, with

$$V_1(x, y) = \begin{cases} U_1(x_1, y_1) := \frac{1}{2}m\omega_1^2(x_1^2 + g^2y_1^2) & \text{if } -\infty < x < 0, -\infty < y < \infty \\ 0 & \text{otherwise} \end{cases}, \quad (4a)$$

$$V_2(x, y) = \begin{cases} U_2(x_2, y_2) := \frac{1}{2}m\omega_2^2(x_2^2 + g^2y_2^2) & \text{if } 0 \leq x < \infty, -\infty < y < \infty \\ 0 & \text{otherwise} \end{cases}, \quad (4b)$$

and the proton wavefunction, $\Psi(x, y, t)$, evolves in time according to the Schrödinger equation,

$$i\hbar \frac{d\Psi}{dt} = \left[-\frac{\hbar^2}{2m} (\partial_x^2 + \partial_y^2) + V \right] \Psi. \quad (5)$$

In eqs. (4) and (5), m is proton mass, ω_1 and ω_2 respectively are natural angular frequencies of the single oscillators U_1 and U_2 , and $g > 0$ is an *isotropy parameter* which we assume to be the same for U_1 and U_2 . We define the *symmetry parameter*,

$$\gamma := \omega_2/\omega_1 \leq 1, \quad (6)$$

so that if $\gamma < 1$ then there is a lower ground state in U_2 than in U_1 , and this represents the fact that the proton's preferred equilibrium is in U_2 . V is a double oscillator which is identical to U_1 to the left of the line $x = 0$ and identical to U_2 to the right of $x = 0$. Thus, there is a potential barrier along the line $x = 0$ where, in general, we have $U_1 \neq U_2$, so that there is a discontinuity in V .

With the potential function in place, we now calculate λ . In the $O_1x_1y_1$ frame, the local potential well's equipotential curve through the point O is an ellipse, with equation $x_1^2 + g^2y_1^2 = 2U_0/(m\omega_1^2)$, where U_0 is the potential energy at O . One could write a similar ellipse equation, in terms of (x_2, y_2) , for the equipotential curve through O in U_2 . Instead, using eqs. (1) and (2), we write both ellipse equations in the Oxy frame, as follows.

$$[(x + \lambda D_\theta) \cos \theta_1 - y \sin \theta_1]^2 + g^2 [(x + \lambda D_\theta) \sin \theta_1 + y \cos \theta_1]^2 = \frac{2U_0}{m\omega_1^2}, \quad (7a)$$

$$[(x - (1 - \lambda) D_\theta) \cos \theta_2 - y \sin \theta_2]^2 + g^2 [(x - (1 - \lambda) D_\theta) \sin \theta_2 + y \cos \theta_2]^2 = \frac{2U_0}{m\omega_2^2}. \quad (7b)$$

Since the ellipses intersect at O, we set $(x, y) = (0, 0)$ in eqs. (7a) and (7b), to obtain

$$U_0 = \frac{m\omega_1^2}{2} \lambda^2 D_\theta^2 (\cos^2 \theta_1 + g^2 \sin^2 \theta_1) = \frac{m\omega_2^2}{2} (1 - \lambda)^2 D_\theta^2 (\cos^2 \theta_2 + g^2 \sin^2 \theta_2), \quad (8)$$

from which it follows that

$$\lambda = \left(1 + \frac{1}{\gamma} \sqrt{\frac{\cos^2 \theta_1 + g^2 \sin^2 \theta_1}{\cos^2 \theta_2 + g^2 \sin^2 \theta_2}} \right)^{-1}. \quad (9)$$

We proceed to compute the characteristic time-scale of proton tunnelling from being localised in U_2 to being localised in U_1 , using the Rayleigh-Ritz ansatz [9], in which the ground state wavefunction of the proton is approximately

$$\Psi(x, y, t) = \alpha_1(t) \phi_1(x, y) + \alpha_2(t) \phi_2(x, y), \quad (10)$$

where $\alpha_{1,2}$ are complex coefficients, and $\phi_{1,2}$ are normalised ground state wavefunctions that the proton would have if it existed in the single-well potential U_1 or U_2 , with their domains extended to the infinite plane. We note that if a proton were in the single oscillator U_1 or U_2 , then its ground state energy would be

$$E_1 := \hbar\omega_1(1 + g)/2 \text{ for } U_1 \quad \text{or} \quad E_2 := \hbar\omega_2(1 + g)/2 \text{ for } U_2, \quad (11)$$

so that the symmetry parameter, γ , equals the energy ratio E_2/E_1 . Scaling length by

$$x_0 := \sqrt{\frac{\hbar}{m\omega_1}}, \quad (12)$$

we have ϕ_1 and ϕ_2 in the following dimensionless forms, in terms of coordinates $\xi_{1,2} := x_{1,2}/x_0$ and $\eta_{1,2} := y_{1,2}/x_0$.

$$\phi_1(\xi_1, \eta_1) = \frac{g^{1/4}}{\sqrt{\pi}} \exp \left[-\frac{1}{2} (\xi_1^2 + g\eta_1^2) \right], \quad -\infty < \xi_1, \eta_1 < \infty, \quad (13a)$$

$$\phi_2(\xi_2, \eta_2) = \frac{g^{1/4}\sqrt{\gamma}}{\sqrt{\pi}} \exp \left[-\frac{\gamma}{2} (\xi_2^2 + g\eta_2^2) \right], \quad -\infty < \xi_2, \eta_2 < \infty. \quad (13b)$$

Scaling time by ω_1^{-1} , then Ψ evolves according to the dimensionless Schrödinger equation,

$$i \frac{d\Psi}{d\tau} = \hat{H}\Psi, \quad (14)$$

where τ is dimensionless time and, in coordinates $(\xi, \eta) = (x, y)/x_0$, we have

$$\hat{H} = \frac{1}{\hbar\omega_1} \left[-\frac{\hbar^2}{2m} (\partial_x^2 + \partial_y^2) + V \right] = -\frac{1}{2} (\partial_\xi^2 + \partial_\eta^2) + v_1 + v_2, \quad (15)$$

with

$$v_1(\xi, \eta) = \begin{cases} u_1(\xi_1, \eta_1) := \frac{1}{2} (\xi_1^2 + g^2 \eta_1^2) & \text{if } -\infty < \xi < 0, -\infty < \eta < \infty \\ 0 & \text{otherwise} \end{cases}, \quad (16a)$$

$$v_2(\xi, \eta) = \begin{cases} u_2(\xi_2, \eta_2) := \frac{\gamma^2}{2} (\xi_2^2 + g^2 \eta_2^2) & \text{if } 0 \leq \xi < \infty, -\infty < \eta < \infty \\ 0 & \text{otherwise} \end{cases}. \quad (16b)$$

Since $\partial_\xi^2 + \partial_\eta^2 = \partial_{\xi_{1,2}}^2 + \partial_{\eta_{1,2}}^2$, we have the following identities.

$$\widehat{H}\phi_1 = \left(\frac{1}{2}(1+g) - u_1 + v_1 + v_2 \right) \phi_1, \quad \widehat{H}\phi_2 = \left(\frac{\gamma}{2}(1+g) - u_2 + v_1 + v_2 \right) \phi_2, \quad (17)$$

where $u_{1,2}$ and $\phi_{1,2}$ are expressed in terms of coordinates (ξ, η) as follows. Defining

$$\Delta_\theta := D_\theta/x_0, \quad (18)$$

and using the dimensionless version of eq. (1), we obtain, for $j = 1, 2$,

$$u_j = \frac{1}{2} (a_j \xi^2 + b_j \eta^2 + 2c_j \xi \eta + 2p_j \xi + 2q_j \eta + r_j), \quad (19)$$

where

$$a_1 = \cos^2 \theta_1 + g^2 \sin^2 \theta_1, \quad a_2 = \gamma^2 (\cos^2 \theta_2 + g^2 \sin^2 \theta_2), \quad (20a)$$

$$b_1 = \sin^2 \theta_1 + g^2 \cos^2 \theta_1, \quad b_2 = \gamma^2 (\sin^2 \theta_2 + g^2 \cos^2 \theta_2), \quad (20b)$$

$$c_1 = (g^2 - 1) \cos \theta_1 \sin \theta_1, \quad c_2 = \gamma^2 (g^2 - 1) \cos \theta_2 \sin \theta_2, \quad (20c)$$

$$p_1 = a_1 \lambda \Delta_\theta, \quad p_2 = -a_2 (1 - \lambda) \Delta_\theta, \quad (20d)$$

$$q_1 = c_1 \lambda \Delta_\theta, \quad q_2 = -c_2 (1 - \lambda) \Delta_\theta, \quad (20e)$$

$$r_1 = a_1 \lambda^2 \Delta_\theta^2, \quad r_2 = a_2 (1 - \lambda)^2 \Delta_\theta^2. \quad (20f)$$

We note that λ [cf. eq. (9)] can now be written

$$\lambda = \left(1 + \sqrt{a_1/a_2} \right)^{-1}, \quad (21)$$

from which it follows that $r_1 = r_2$. We therefore define

$$r_0 := r_1 = r_2 = \frac{a_1 a_2 \Delta_\theta^2}{(\sqrt{a_1} + \sqrt{a_2})^2}. \quad (22)$$

For ϕ_j with $j = 1, 2$, we have, for $-\infty < \xi, \eta < \infty$,

$$\phi_j(\xi, \eta) = \frac{g^{1/4}}{\sqrt{\pi}} \gamma^{\frac{j-1}{2}} \exp \left[-\frac{1}{2} (A_j \xi^2 + B_j \eta^2 + 2C_j \xi \eta + 2P_j \xi + 2Q_j \eta + R_j) \right], \quad (23)$$

where

$$A_1 = \cos^2 \theta_1 + g \sin^2 \theta_1, \quad A_2 = \gamma (\cos^2 \theta_2 + g \sin^2 \theta_2), \quad (24a)$$

$$B_1 = \sin^2 \theta_1 + g \cos^2 \theta_1, \quad B_2 = \gamma (\sin^2 \theta_2 + g \cos^2 \theta_2), \quad (24b)$$

$$C_1 = (g - 1) \cos \theta_1 \sin \theta_1, \quad C_2 = \gamma (g - 1) \cos \theta_2 \sin \theta_2, \quad (24c)$$

$$P_1 = A_1 \lambda \Delta_\theta, \quad P_2 = -A_2 (1 - \lambda) \Delta_\theta, \quad (24d)$$

$$Q_1 = C_1 \lambda \Delta_\theta, \quad Q_2 = -C_2 (1 - \lambda) \Delta_\theta, \quad (24e)$$

$$R_1 = A_1 \lambda^2 \Delta_\theta^2, \quad R_2 = A_2 (1 - \lambda)^2 \Delta_\theta^2. \quad (24f)$$

Defining the inner product $\langle f | g \rangle := \int_{-\infty}^{\infty} d\xi \int_{-\infty}^{\infty} d\eta f^* g$, we take the inner product of eq. (14) with $\langle \phi_1 |$ and $\langle \phi_2 |$ respectively to obtain

$$i \begin{pmatrix} 1 & S \\ S & 1 \end{pmatrix} \begin{pmatrix} \dot{\alpha}_1 \\ \dot{\alpha}_2 \end{pmatrix} = \begin{pmatrix} H_{11} & H_{12} \\ H_{21} & H_{22} \end{pmatrix} \begin{pmatrix} \alpha_1 \\ \alpha_2 \end{pmatrix}, \quad (25)$$

where the overdot denotes differentiation with respect to τ , and

$$S = \langle \phi_1 | \phi_2 \rangle, \quad H_{jk} = \langle \phi_j | \hat{H} \phi_k \rangle. \quad (26)$$

We note that since ϕ_1, ϕ_2 are positive, square normalised functions, and since $\phi_1 \not\equiv \phi_2$, we have $0 < S < 1$. Next, using eq. (17), we deduce

$$\begin{pmatrix} H_{11} & H_{12} \\ H_{21} & H_{22} \end{pmatrix} = \begin{pmatrix} \frac{1}{2}(1+g) + I_{11} & \frac{\gamma}{2}(1+g)S - I_{12} \\ \frac{1}{2}(1+g)S + I_{21} & \frac{\gamma}{2}(1+g) - I_{22} \end{pmatrix}, \quad (27)$$

where

$$\begin{pmatrix} I_{11} & I_{12} \\ I_{21} & I_{22} \end{pmatrix} = \begin{pmatrix} \int_0^\infty d\xi \int_{-\infty}^\infty d\eta (u_2 - u_1) \phi_1^2 & \int_{-\infty}^0 d\xi \int_{-\infty}^\infty d\eta (u_2 - u_1) \phi_1 \phi_2 \\ \int_0^\infty d\xi \int_{-\infty}^\infty d\eta (u_2 - u_1) \phi_1 \phi_2 & \int_{-\infty}^0 d\xi \int_{-\infty}^\infty d\eta (u_2 - u_1) \phi_2^2 \end{pmatrix}, \quad (28)$$

By invoking the change of variable $\xi \mapsto -\xi$ where necessary, we write, for $j = 1, 2$ and $k = 1, 2$,

$$I_{jk} = \frac{\sqrt{g}}{2\pi} \gamma^{\frac{j+k}{2}-1} \int_0^\infty d\xi \int_{-\infty}^\infty d\eta \left(a\xi^2 + b\eta^2 + 2(-1)^{k-1}c\xi\eta + 2(-1)^{k-1}p\xi + 2q\eta \right) \exp \left[-\frac{1}{2} \left(A_{jk}\xi^2 + B_{jk}\eta^2 + 2(-1)^{k-1}C_{jk}\xi\eta + 2(-1)^{k-1}P_{jk}\xi + 2Q_{jk}\eta + R_{jk} \right) \right], \quad (29)$$

where $a = a_2 - a_1$, $A_{jk} = A_j + A_k$, and analogous definitions hold for $b, B_{jk}, c, C_{jk}, p, P_{jk}, q, Q_{jk}$ and R_{jk} . Each *transition integral* I_{jk} can be evaluated exactly, as can the *overlap integral*, S . We present closed-form expressions for these integrals in the Appendix.

To solve eq. (25) for $\alpha_j(\tau)$, we write

$$\begin{pmatrix} \dot{\alpha}_1 \\ \dot{\alpha}_2 \end{pmatrix} = \begin{pmatrix} J & K \\ M & N \end{pmatrix} \begin{pmatrix} \alpha_1 \\ \alpha_2 \end{pmatrix}, \quad (30)$$

where

$$\begin{pmatrix} J & K \\ M & N \end{pmatrix} = \frac{-i}{1-S^2} \begin{pmatrix} 1 & -S \\ -S & 1 \end{pmatrix} \begin{pmatrix} H_{11} & H_{12} \\ H_{21} & H_{22} \end{pmatrix} = -i \begin{pmatrix} \frac{1}{2}(1+g) + \frac{I_{11}-SI_{21}}{1-S^2} & -\frac{I_{12}-SI_{22}}{1-S^2} \\ \frac{I_{21}-SI_{11}}{1-S^2} & \frac{\gamma}{2}(1+g) - \frac{I_{22}-SI_{12}}{1-S^2} \end{pmatrix}. \quad (31)$$

The solution of eq. (30) subject to the initial condition, $(\alpha_1, \alpha_2) = (0, 1)$ at $\tau = 0$, is

$$\begin{pmatrix} \alpha_1 \\ \alpha_2 \end{pmatrix} = \frac{1}{\mathcal{N}_\tau} (\beta_+ \mathbf{r}_+ e^{\tau\rho_+} + \beta_- \mathbf{r}_- e^{\tau\rho_-}), \quad (32)$$

where

$$\rho_\pm = \frac{J + N \pm \Omega}{2}, \quad \mathbf{r}_\pm = \left(1, \frac{-J + N \pm \Omega}{2K} \right)^T, \quad \beta_\pm = \pm K/\Omega, \quad (33)$$

with

$$\Omega = \sqrt{(J - N)^2 + 4KM}, \quad (34)$$

and we determine the real function \mathcal{N}_τ as follows. From eq. (32), we have

$$\alpha_1 = \frac{2K}{\mathcal{N}_\tau \Omega} \exp\left(\frac{J+N}{2}\tau\right) \sinh \frac{\Omega\tau}{2}, \quad (35a)$$

$$\alpha_2 = \frac{1}{\mathcal{N}_\tau} \exp\left(\frac{J+N}{2}\tau\right) \left[\cosh \frac{\Omega\tau}{2} - \frac{(J-N)}{\Omega} \sinh \frac{\Omega\tau}{2} \right]. \quad (35b)$$

Assume for now that Ω is pure imaginary, which we later verify numerically, then we have

$$\sinh \frac{\Omega\tau}{2} = i \sin \frac{|\Omega|\tau}{2}, \quad \cosh \frac{\Omega\tau}{2} = \cos \frac{|\Omega|\tau}{2}. \quad (36)$$

Since $|e^{(J+N)\tau/2}| = 1$, it follows from the normalisation condition, $\langle \Psi | \Psi \rangle = |\alpha_1|^2 + |\alpha_2|^2 + (\alpha_1^* \alpha_2 + \alpha_2^* \alpha_1)S = 1$, that

$$\mathcal{N}_\tau = \sqrt{\cos^2 \frac{|\Omega|\tau}{2} + \sigma \sin^2 \frac{|\Omega|\tau}{2}}, \quad (37)$$

where $\sigma = (4|K|^2 + |J-N|^2 + 4K(J-N)S)/|\Omega|^2$, which is real because $K(J-N)$ is real. Since $S < 1$, we have $\sigma > (4|K|^2 + |J-N|^2 - 4|K(J-N)|)/|\Omega|^2 = (2|K| - |J-N|)^2/|\Omega|^2$, therefore $\sigma > 0$. In the proton wavefunction $\Psi = \alpha_1 \phi_1 + \alpha_2 \phi_2$, α_2 is initially unity and α_1 is initially zero, so we say that the proton's CTT, the time it takes for Ψ to evolve from being localised as ϕ_2 to being localised as ϕ_1 , is the time at which

$$|\alpha_1| = \frac{2|K|}{\mathcal{N}_\tau |\Omega|} \left| \sin \frac{|\Omega|\tau}{2} \right| \quad (38)$$

first reaches its maximum. This happens at the smallest τ for which the following holds.

$$\begin{aligned} 0 &= \frac{d}{d\tau} \frac{\sin \frac{|\Omega|\tau}{2}}{\mathcal{N}_\tau} = \frac{|\Omega|}{2\mathcal{N}_\tau} \cos \frac{|\Omega|\tau}{2} + \frac{|\Omega|}{2\mathcal{N}_\tau^3} \left(\cos \frac{|\Omega|\tau}{2} \sin \frac{|\Omega|\tau}{2} - \sigma \sin \frac{|\Omega|\tau}{2} \cos \frac{|\Omega|\tau}{2} \right) \sin \frac{|\Omega|\tau}{2} \\ &= \frac{|\Omega|}{2\mathcal{N}_\tau^3} \cos \frac{|\Omega|\tau}{2}. \end{aligned} \quad (39)$$

Therefore, the CTT of the proton, in units of seconds, is

$$t_p = \frac{\pi}{\omega_1 |\Omega|}, \quad (40)$$

where, due to eqs. (31) and (34), we have

$$\Omega = \sqrt{- \left[\frac{1}{2} (1+g)(1-\gamma) + \frac{I_{11} + I_{22} - S(I_{12} + I_{21})}{1 - S^2} \right]^2 + \frac{4(I_{12} - SI_{22})(I_{21} - SI_{11})}{(1 - S^2)^2}}. \quad (41)$$

We have the following values for the parameters D_0, L and g which are appropriate for H bonds across the DNA double helix [10–13]. $4.5 \times 10^{14} \text{ s}^{-1} \leq \omega_1 \leq 6.4 \times 10^{14} \text{ s}^{-1}$, $0.61 \text{ \AA} \leq D_0 \leq 0.81 \text{ \AA}$, $1.03 \text{ \AA} \leq L \leq 1.07 \text{ \AA}$, $g \approx 0.5$. We fix $\omega_1 = 5.45 \times 10^{14} \text{ s}^{-1}$, $D_0 = 0.71 \text{ \AA}$, $L = 1.05 \text{ \AA}$, $g = 0.5$, and compute t_p as functions of the parameters γ, d_x, d_y and θ . For all parameter values which we have studied, we find $\Omega^2 < 0$, which ensures that eq. (36) holds. We note also that when $\gamma = 1$, we recover results of [8] relating to deformations of a *symmetric* double oscillator.

In order for our model to represent tunnelling, rather than scattering, we must have the height U_0 [cf. eq. (8)] of the saddle point in the double-well potential surface being greater than the ground-state energy of ϕ_2 [cf. eq. (11)]; that is, we must have

$$u_0 := \frac{U_0}{E_2} = \frac{r_0}{\gamma(1+g)} > 1. \quad (42)$$

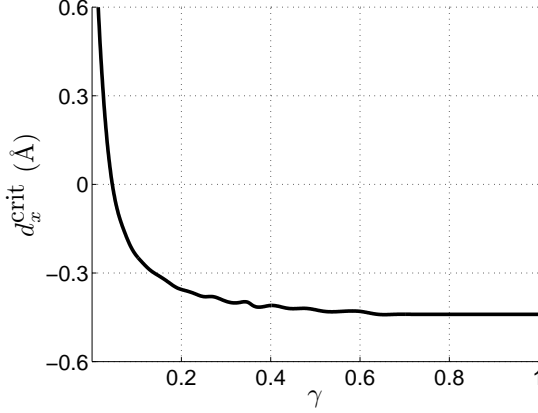


Figure 2: d_x^{crit} as a function of γ .

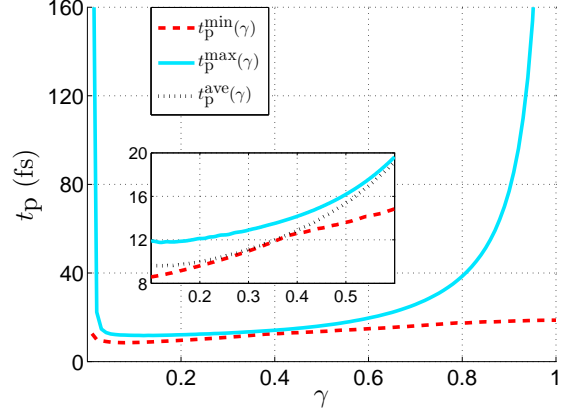


Figure 3: Min, max, average t_p as functions of γ .

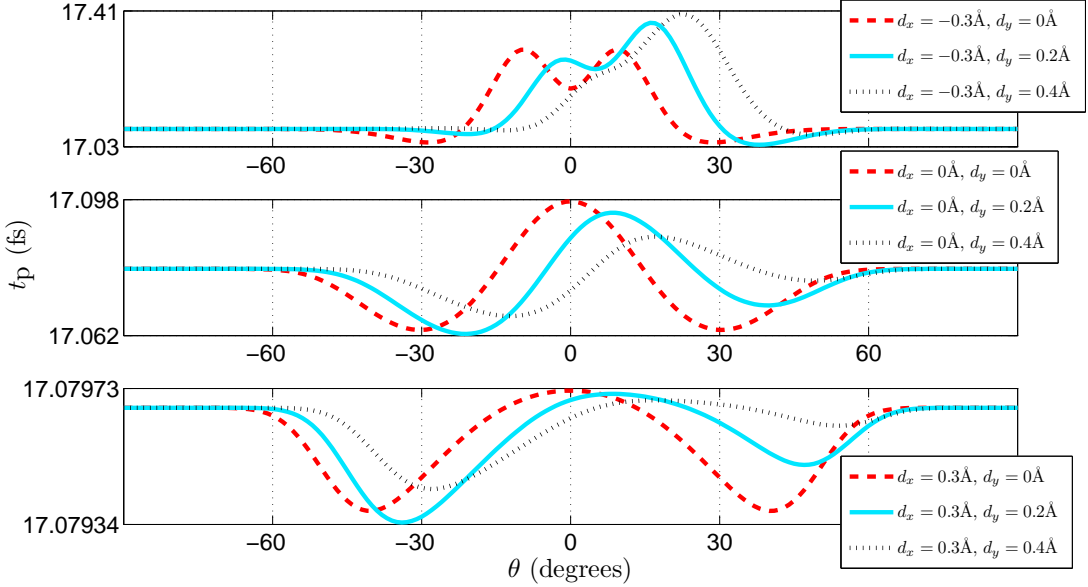
The deformation parameters d_x, d_y and θ are encoded in r_0 , as per the definition of eq. (22). Our results show that, for each value of γ , there exists some critical value d_x^{crit} such that, if $d_x \geq d_x^{\text{crit}}$ then eq. (42) is satisfied given any combination of (d_y, θ) , whereas if $d_x < d_x^{\text{crit}}$ then there are some combinations of (d_y, θ) under which eq. (42) fails to hold. Figure 2 shows d_x^{crit} as a function of γ . As γ decreases towards 0, greater values of d_x would be needed in order to guarantee that every combination of (d_y, θ) produces a valid tunnelling model. This is because γ is positively correlated with the steepness of the local potential well $U_2(x_2, y_2)$. The smaller γ is, the further away from $(x_2, y_2) = (0, 0)$ one needs to go before U_2 reaches the required height, namely the ground-state energy of ϕ_2 ; thus, in order to ensure that the saddle point between U_1 and U_2 is sufficiently high, U_1 and U_2 must be far enough apart, hence the large d_x^{crit} . Meanwhile, as $\gamma \rightarrow 1$, we observe that $d_x^{\text{crit}} \rightarrow -0.44 \text{ \AA}$.

For $0.01 \leq \gamma \leq 1$, we vary d_x, d_y, θ as follows. $-0.45 \text{ \AA} \leq d_x, d_y \leq 0.45 \text{ \AA}$, $-90^\circ \leq \theta \leq 90^\circ$, and we only consider combinations of $(\gamma, d_x, d_y, \theta)$ such that eq. (42) holds. We find that for each γ , t_p falls in a range between some $t_p^{\text{min}}(\gamma)$ and some $t_p^{\text{max}}(\gamma)$, and in Figure 3 we present these extremal values as functions of γ . Crucially, our results show that for $0.01 \leq \gamma \leq 0.99$, we always have $8.5 \text{ fs} \leq t_p(\gamma, d_x, d_y, \theta) \leq 770 \text{ fs}$. We also observe that $t_p^{\text{max}}(\gamma)$ increases steeply both as $\gamma \rightarrow 0$ and as $\gamma \rightarrow 1$. Indeed, when $\gamma = 1$, $t_p^{\text{max}}(\gamma)$ becomes $\sim \mathcal{O}(10^{27}) \text{ s}$; and even though $t_p^{\text{min}}(\gamma)$ is still $\sim \mathcal{O}(10^{-14}) \text{ s}$, t_p increases rapidly as (d_x, d_y, θ) moves away from the combination which minimises t_p . Moreover, $t_p^{\text{min}}(\gamma)$ is slowly varying with γ , and there is a range of values of γ , namely $0.2 \lesssim \gamma \lesssim 0.4$, for which $t_p^{\text{min}}(\gamma)$ becomes close to $t_p^{\text{max}}(\gamma)$. In this case, varying (d_x, d_y, θ) has little effect on t_p , which contrasts strongly with the large- γ and small- γ cases where t_p is very sensitive to (d_x, d_y, θ) . We have defined $t_p^{\text{ave}}(\gamma)$ as the mean t_p , given a fixed γ , over all combinations of (d_x, d_y, θ) which satisfy eq. (42), and we have presented $t_p^{\text{ave}}(\gamma)$ for $0.1 \leq \gamma \leq 0.6$ in the small box in Figure 3. As $\gamma \rightarrow 1$, we have $t_p^{\text{ave}}(\gamma) \sim t_p^{\text{max}}(\gamma)$, and for intermediate values of γ , namely $\gamma \approx 0.3$, we have $t_p^{\text{ave}}(\gamma) \sim t_p^{\text{min}}(\gamma)$, but as $\gamma \rightarrow 0$, $t_p^{\text{ave}}(\gamma)$ is asymptotic to neither $t_p^{\text{min}}(\gamma)$ nor $t_p^{\text{max}}(\gamma)$.

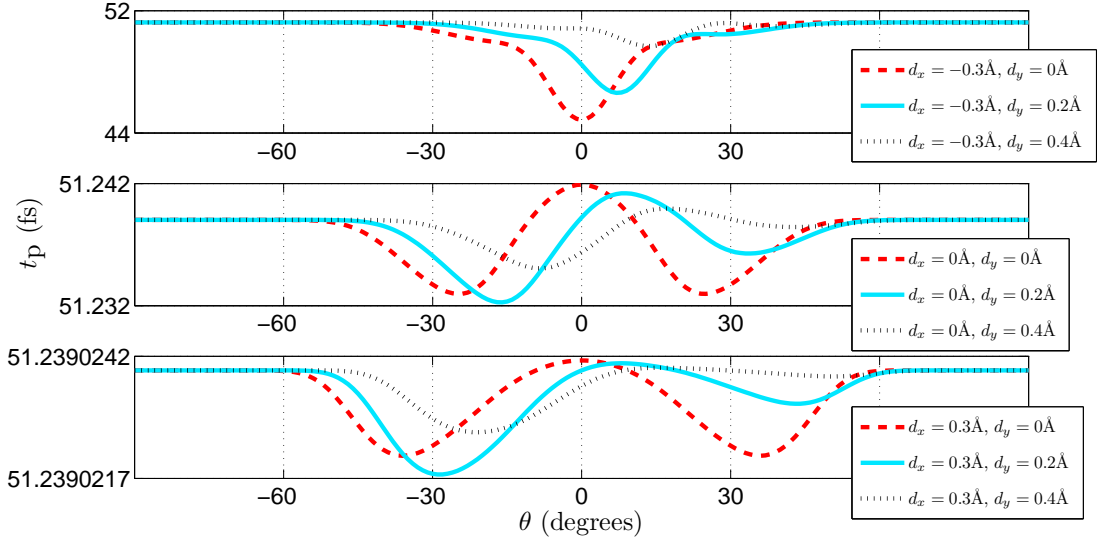
Furthermore, our results show that for every (γ, d_x) , we have

$$t_p(\gamma, d_x, d_y, \theta) = t_p(\gamma, d_x, -d_y, -\theta). \quad (43)$$

This is because a deformation consisting of a shift of d_y and rotation of θ is intrinsically identical to one consisting of a shift and rotation of the same magnitudes but both in the opposite direction. Figure 4 shows variations in t_p as θ varies between -90° and 90° , whilst (γ, d_x, d_y) are fixed at certain values. For every combination of (γ, d_x) , we have presented only results relating to $d_y \geq 0$, since one can simply reflect these curves about $\theta = 0$ to obtain results for $d_y < 0$. For fixed (γ, d_x) with $d_y = 0$, the graph of $t_p(\theta)$ is symmetric about $\theta = 0$, where



(a) $\gamma = 0.55$.



(b) $\gamma = 0.85$.

Figure 4: t_p as functions of θ , given various combinations of (γ, d_x, d_y) .

the graph has a local minimum under some (γ, d_x) and a local maximum under others; we find from our results that for every γ there is one value of d_x at which the graph transitions from having a local minimum to having a local maximum at $\theta = 0$, and that this value of d_x increases with γ . For fixed (γ, d_x) with $d_y \neq 0$, the symmetry of $t_p(\theta)$ about $\theta = 0$ is broken, and as d_y increases, the local extremum which was at $\theta = 0$ when $d_y = 0$ moves towards larger θ . There are cases where this local extremum ceases to exist when d_y becomes large, for instance the case of $(\gamma, d_x) = (0.55, -0.3\text{\AA})$, as we can see in Figure 4a: there is a local minimum at $\theta = 0$ if $d_y = 0$ and at $\theta = 5^\circ$ if $d_y = 0.2\text{\AA}$, but if $d_y = 0.4\text{\AA}$ then this local minimum disappears. For any fixed (γ, d_x, d_y) , we always have t_p tending to some value as θ tends to $\pm 90^\circ$, typically with several local extrema between $\theta = 0$ and $\theta = \pm 90^\circ$; the value of this limit at $\pm 90^\circ$ is dependent only on γ . Calling this limit $t_p^{90}(\gamma)$, we have $t_p^{90}(0.55) = 17.1\text{fs}$, and $t_p^{90}(0.85) = 51.2\text{fs}$. As $\gamma \rightarrow 1$ and as $\gamma \rightarrow 0$, we have $t_p^{90}(\gamma) \sim t_p^{\max}(\gamma)$, and for $0.02 \lesssim \gamma \lesssim 0.4$, we have $t_p^{90}(\gamma) \sim t_p^{\min}(\gamma)$.

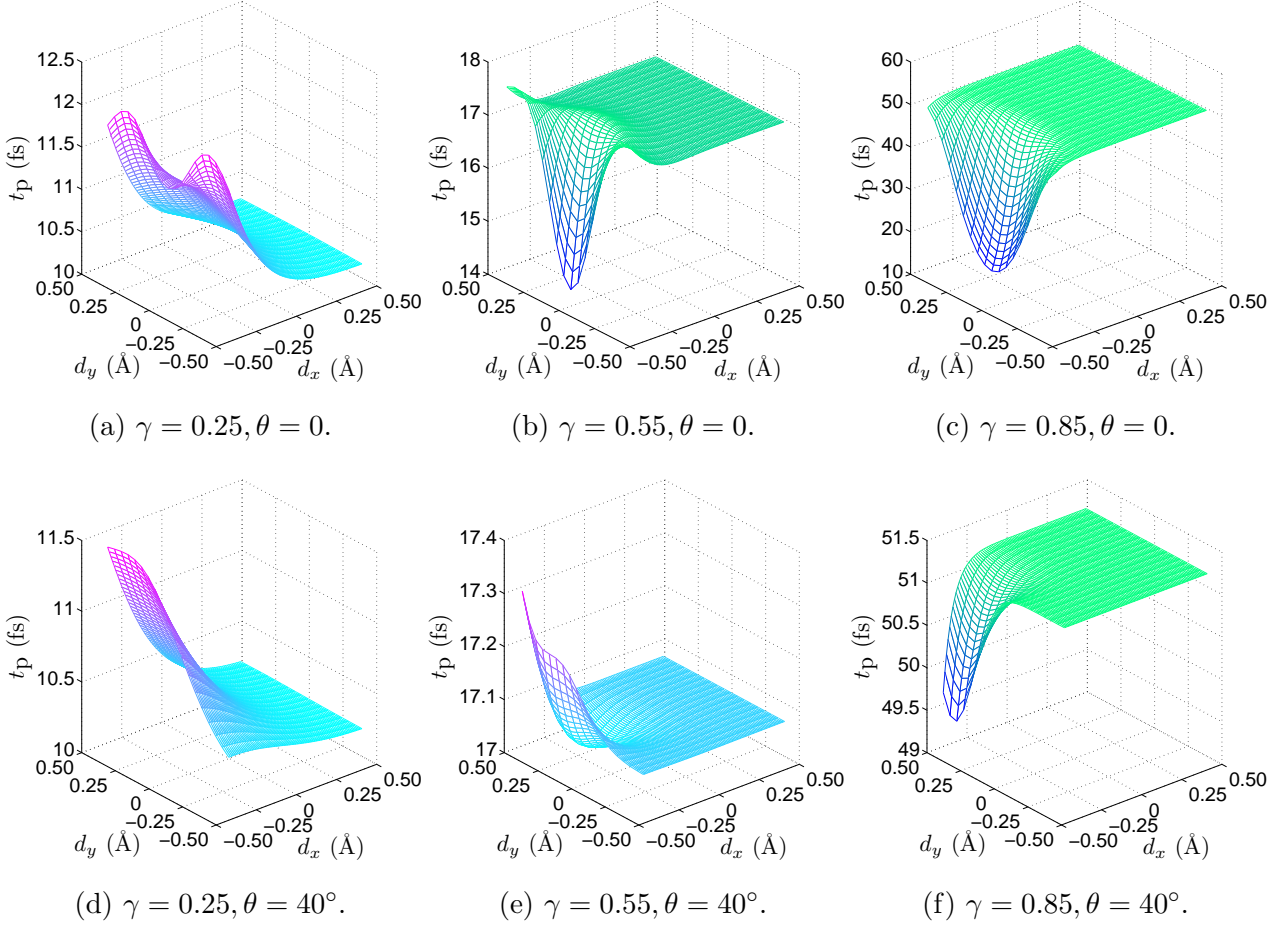


Figure 5: t_p as surfaces over the parameter subspace (d_x, d_y) , given various combinations of (γ, θ) . In each case, the range of d_x is $d_x^{\text{crit}} \leq d_x \leq 0.45\text{\AA}$.

We further observe by comparing Figures 4a and 4b that, when $\gamma = 0.85$, there is a larger overall variation in t_p as a result of varying (d_x, d_y, θ) , compared to when $\gamma = 0.55$. This agrees with our observation about Figure 3 that the gap between $t_p^{\min}(\gamma)$ and $t_p^{\max}(\gamma)$ increases as $\gamma \rightarrow 1$. Indeed, this gap also increases as $\gamma \rightarrow 0$. Moreover, for fixed γ , the larger d_x is, the less t_p varies with θ or with d_y . As we see in Figures 5b, 5c, 5e and 5f, if γ is far from 0, then for fixed (γ, θ) , t_p as a surface over (d_x, d_y) is almost constant given sufficiently large d_x . As $d_x \rightarrow \infty$, t_p always tends to some limit, whose value is independent of d_y . Meanwhile, we see in Figures 5a to 5c that if $\theta = 0$, then for fixed (γ, θ) , t_p as a surface over (d_x, d_y) is symmetric about the line $d_y = 0$. This is due to eq. (43). If $\theta = 0$ and γ is moderate, such as 0.55, then for each d_y sufficiently to 0 we have some small value of d_x which maximises t_p , as we can see in Figure 5b. This shows that increasing d_x , which represents moving the donor away from the acceptor in the H bond, does not necessarily prolong the proton tunnelling. If $\theta \neq 0$, then the symmetry about $d_y = 0$ is broken, and reflecting a surface for $\theta > 0$ about the line $d_y = 0$ produces corresponding results for $\theta < 0$.

3 Discussions and Conclusions

We have studied the quantum mechanical tunnelling of a proton across the potential barrier between the donor and acceptor of a planar hydrogen bond in DNA, and computed an analytical expression for the proton's characteristic tunnelling time (CTT) as a function of four

parameters describing the geometry of the bond. Three of these parameters, d_x, d_y and θ , represent the deformation of the H bond from its normal alignment, under the assumption that any deformation consists of planar translations and rotations of the donor and acceptor molecules as independent units. With the acceptor molecule treated without loss of generality as fixed, d_x and d_y respectively represent the longitudinal and lateral displacements of the donor molecule from its normal position, while θ represents the rotation of the donor molecule about the donor atom from its normal orientation. The fourth parameter, γ , taking values $0 < \gamma \leq 1$, represent the intrinsic symmetry that the potential in the H bond possesses when the bond is in its normal alignment. When $\gamma = 1$, we recover a model previously studied in [8], whose potential function in the normal H bond was symmetric about the potential barrier, so that the local potential wells near the donor and acceptor are equivalent to each other. This symmetry is broken only if some of (d_x, d_y, θ) is non-zero. For $0 < \gamma < 1$, the symmetry is broken even if $d_x = d_y = \theta = 0$, in the sense that the local potential well near the donor has a less energetic ground state than the one near the acceptor, and this gives a better representation of the physical property of the H bond than $\gamma = 1$. In addition, setting any of d_x, d_y and θ to non-zero values further distorts the symmetry between the two local potential wells.

We have discovered that some combinations of $(\gamma, d_x, d_y, \theta)$ provide potential functions which cannot model a tunnelling process, because the potential barrier is not higher than the ground state energy of a proton in equilibrium near the donor. The smaller γ is, the more (d_x, d_y, θ) combinations provide invalid models, meaning that the region of validity in our parameter space shrinks as γ decreases. For $0.01 \leq \gamma \leq 0.99, -0.45\text{\AA} \leq d_x, d_y \leq 0.45\text{\AA}, -90^\circ \leq \theta \leq 90^\circ$, and excluding all invalid parameter combinations, we have found that $8.5\text{fs} \leq t_p(\gamma, d_x, d_y, \theta) \leq 770\text{fs}$, where t_p stands for the proton's CTT. For each γ , certain (d_x, d_y, θ) combinations minimise or maximise t_p , and we have found that $t_p^{\min}(\gamma)$ is a slowly-varying function taking values around 10fs, whilst $t_p^{\max}(\gamma)$ diverges as $\gamma \rightarrow 0$ and grows rapidly towards $\mathcal{O}(10^{27})\text{s}$ as $\gamma \rightarrow 1$. Taking the mean t_p over all (d_x, d_y, θ) for every fixed γ , we have found that $t_p^{\text{ave}}(\gamma) \sim t_p^{\max}(\gamma)$ as $\gamma \rightarrow 1$. This means that in an H bond selected at random from a statistical ensemble, the proton's CTT is likely to be as large as it can be if the potential in the bond has a high γ -symmetry. On the other hand, we have also observed that if γ takes moderate values such as $\gamma \approx 0.3$, then $t_p^{\text{ave}}(\gamma) \sim t_p^{\min}(\gamma)$, meaning that the proton's CTT is likely to be as small as it can be in this case. As $\gamma \rightarrow 0$, $t_p^{\text{ave}}(\gamma)$ is not asymptotic to $t_p^{\min}(\gamma)$ or $t_p^{\max}(\gamma)$; given the fact that $t_p^{\max}(\gamma)$ diverges towards infinity in this case, we deduce that parameter combinations resulting in large t_p are rare when γ is small. We have investigated how t_p varies with θ given fixed (γ, d_x, d_y) , and found that as $\theta \rightarrow \pm 90^\circ$, t_p always converges to some $t_p^{90}(\gamma)$ which depends on γ in the following manner. In extreme cases of $\gamma \rightarrow 1$ and $\gamma \rightarrow 0$, we have $t_p^{90}(\gamma) \sim t_p^{\max}(\gamma)$, and for moderate γ values, we have $t_p^{90}(\gamma) \sim t_p^{\min}(\gamma)$. For $-90^\circ < \theta < 90^\circ$, we have observed that t_p has various local maxima and local minima but the variation in t_p is small unless either γ is close to extremal values, or d_x is negative with large magnitudes. For example, if $0.3 \leq \gamma \leq 0.99$ and $d_x \geq 0$, then regardless of d_y , we have the result that as θ varies, t_p never deviates by more than 1% from some average value. We have also investigated how t_p varies with (d_x, d_y) , given fixed (γ, θ) , and found that if d_x is sufficiently large, then t_p is an almost-constant surface over (d_x, d_y) , and that t_p tends to some d_y -independent limit as $d_x \rightarrow \infty$. Since large d_x corresponds to large donor-acceptor separation, one might expect t_p to be maximised in the limit $d_x \rightarrow \infty$, but our results show that this is not always the case.

The most important difference that generalising from $\gamma = 1$ to $0 < \gamma \leq 1$ has made is that, for most γ values in $0 < \gamma < 1$, the proton CTT is sub-picosecond regardless of (d_x, d_y, θ) . Compared to the $\gamma = 1$ case in which some (d_x, d_y, θ) give CTTs of $\mathcal{O}(10^{27})\text{s}$, the sub-picosecond time-scale is much more biologically relevant. Moreover, if γ is such that the CTT is guaranteed to be sub-picosecond, then it varies by no more than 2 orders of magnitude as the H bond

deforms. This means that the tunnelling process is much more stable with respect to bond deformation compared to the $\gamma = 1$ case, under which the CTT varies by over 30 orders of magnitude as the H bond deforms. Overall, our model under moderate γ -values produces CTTs on a biological time-scale with strong stability against bond deformation, and therefore it supports the theory that proton tunnelling across DNA hydrogen bonds may be a mechanism responsible for biological processes such as spontaneous mutation.

Appendix

In Section 2 we presented the overlap integral S and transition integrals I_{jk} , for $j, k = 1, 2$ [cf. eqs. (26) and (29)]. We have computed closed-form expressions for these integrals, as follows.

$$S = 2 \frac{\sqrt{g\gamma}}{K_{0,12}} \exp \left[K_{1,12} + \frac{K_{2,12}^2}{2B_{12}K_{0,12}^2} \right], \quad (44a)$$

$$I_{jk} = \sqrt{g\gamma}^{\frac{j+k}{2}-1} \left[\left(\frac{bQ_{jk}^2}{B_{jk}^2} + \frac{b-2qQ_{jk}}{B_{jk}} \right) J_{0,jk} \right. \\ \left. + 2(-1)^{k-1} \left(\frac{bC_{jk}Q_{jk}}{B_{jk}^2} - \frac{(cQ_{jk} + qC_{jk})}{B_{jk}} + p \right) J_{1,jk} \right. \\ \left. + \left(\frac{bC_{jk}^2}{B_{jk}^2} - \frac{2cC_{jk}}{B_{jk}} + a \right) J_{2,jk} \right], \quad (44b)$$

where

$$J_{0,jk} = \frac{1}{2K_{0,jk}} \exp \left(K_{1,jk} + \frac{K_{2,jk}^2}{2B_{jk}K_{0,jk}^2} \right) \operatorname{erfc} \left(\frac{K_{2,jk}}{(-1)^{k-1}\sqrt{2B_{jk}}K_{0,jk}} \right), \quad (45a)$$

$$J_{1,jk} = \frac{\sqrt{B_{jk}}}{\sqrt{2\pi}K_{0,jk}^2} \exp(K_{1,jk}) \\ + (-1)^k \frac{K_{2,jk}}{2K_{0,jk}^3} \exp \left(K_{1,jk} + \frac{K_{2,jk}^2}{2B_{jk}K_{0,jk}^2} \right) \operatorname{erfc} \left(\frac{K_{2,jk}}{(-1)^{k-1}\sqrt{2B_{jk}}K_{0,jk}} \right), \quad (45b)$$

$$J_{2,jk} = (-1)^k \frac{\sqrt{B_{jk}}K_{2,jk}}{\sqrt{2\pi}K_{0,jk}^4} \exp(K_{1,jk}) \\ + \frac{\left(K_{2,jk}^2 + B_{jk}K_{0,jk}^2 \right)}{2K_{0,jk}^5} \exp \left(K_{1,jk} + \frac{K_{2,jk}^2}{2B_{jk}K_{0,jk}^2} \right) \operatorname{erfc} \left(\frac{K_{2,jk}}{(-1)^{k-1}\sqrt{2B_{jk}}K_{0,jk}} \right), \quad (45c)$$

with

$$K_{0,jk} = \sqrt{A_{jk}B_{jk} - C_{jk}^2}, \quad K_{1,jk} = \frac{Q_{jk}^2}{2B_{jk}} - \frac{R_{jk}}{2}, \quad K_{2,jk} = B_{jk}P_{jk} - C_{jk}Q_{jk}, \quad (46)$$

and erfc being the cumulative error function, defined for all real X by

$$\operatorname{erfc}(X) = (2/\sqrt{\pi}) \int_X^\infty e^{-z^2} dz. \quad (47)$$

The parameters $a, b, c, p, q, A_{jk}, B_{jk}, C_{jk}, P_{jk}, Q_{jk}, R_{jk}$ were defined in the main text.

Acknowledgement

The author is grateful to Dr. Emma Coutts and Dr. Bernard Piette for their generous and helpful suggestions.

References

- [1] L. Pauling. *The Nature of the Chemical Bond*. Cornell University Press, 3rd edition, 1960.
- [2] E. Arunan, G. R. Desiraju, R. A. Klein, J. Sadlej, S. Scheiner, I. Alkorta, D. C. Clary, R. H. Crabtree, J. J. Dannenberg, P. Hobza, H. G. Kjaergaard, A. C. Legon, B. Mennucci, and D. J. Nesbitt. *Pure Appl. Chem.*, 83:1637, 2011.
- [3] P.-O. Löwdin. *Rev. Mod. Phys.*, 35:724, 1963.
- [4] J. McFadden and J. Al-Khalili. *BioSystems*, 50:203, 1999.
- [5] R. E. Dickerson. *Nucleic Acids Research*, 17:1797, 1989.
- [6] X.-J. Lu and Wilma. K. Olson. *J Mol. Biol.*, 285:1563, 1999.
- [7] W. K. Olson, M. Bansal, S. K. Burley, R. E. Dickerson, M. Gerstein, S. C. Harvey, U. Heinemann, X.-J. Lu, S. Neidle, Z. Shakked, H. Sklenar, M. Suzuki, C.-S. Tung, E. Westhof, C. Wolberger, and H. M. Berman. *J. Mol. Biol.*, 313:229, 2001.
- [8] P. M. Krasilnikov. *Biophysics*, 59:189, 2014.
- [9] E. Merzbacher. *Quantum Mechanics*. Wiley, 3rd edition, 1998.
- [10] S. Ia. Ishenko, M. V. Vener, and V. M. Mamaev. *Theor. Chim. Acta*, 68:351, 1985.
- [11] R. Santamaria, E. Charro, A. Zacarías, and M. Castro. *J. Comput. Chem.*, 20:511, 1999.
- [12] C. Fonseca Guerra, F. M. Bickelhaupt, J. G. Snijders, and E. J. Baerends. *J. Am. Chem. Soc.*, 122:4117, 2000.
- [13] T. Steiner. *Angew. Chem. Int. Ed.*, 41:48, 2002.